

Optimizing Stability through Conformational Locking and Ring Fusion Modulations in Organic Semiconductors

Salahuddin S. Attar,^a Bahattin Bademci,^b Maciej Bartóg,^a Dusan Seredjovic,^{a, c} Hessa Al-Thani,^a Sandra Dudley,^b Konstantinos Kakosimos,^a Hassan S. Bazzi,^d Muhammad Tariq Sajjad,^{b*} and Mohammed Al-Hashimi^{a*}

^a Department of Chemical Engineering, Texas A&M University at Qatar, P.O. Box 23874, Doha, Qatar

^b School of Engineering, London South Bank University, 103 Borough Road, London, SE1 0AA, United Kingdom.

^c Vinča Institute of Nuclear Sciences – National Institute of the Republic of Serbia, University of Belgrade, Centre of Excellence for Photoconversion, P.O. Box 522, 11001 Belgrade, Serbia

^d Division of Arts and Science, Texas A&M University at Qatar, Education City, Doha, P.O. Box 23874, Qatar.

Contents

1. Materials and characterization	3
2. Synthetic Procedures :	4
2.1. Synthesis of tert-butyl (2-bromothiophen-3-yl)carbamate.....	4
2.2. Synthesis of tert-butyl (2-(trimethylstannyl)thiophen-3-yl)carbamate.....	5
2.3. Synthesis of di-tert-butyl ((5,7-bis(2-ethylhexyl)-4,8-dioxo-4H,8H-benzo[1,2-c:4,5-c']dithiophene-1,3-diyl)bis(thiophene-2,3-diyl))dicarbamate	6
2.4. Synthesis of di-tert-butyl ((5,7-bis(2-decyltetradecyl)-4,8-dioxo-4H,8H-benzo[1,2-c:4,5-c']dithiophene-1,3-diyl)bis(thiophene-2,3-diyl))dicarbamate	7
2.5. Synthesis of 5,7-bis(2-ethylhexyl)tetrathieno[2,3-b:3',4'-f:3'',2''-j:2''',3''',4''',5'''-lmn][4,7]phenanthroline	7
2.6. Synthesis of 5,7-bis(2-decyltetradecyl)tetrathieno[2,3-b:3',4'-f:3'',2''-j:2''',3''',4''',5'''-lmn][4,7]phenanthroline	8
2.7. Synthesis of 5,7-bis(2-decyltetradecyl)-2,10-bis(trimethylstannyl)tetrathieno[2,3-b:3',4'-f:3'',2''-j:2''',3''',4''',5'''-lmn][4,7]phenanthroline	9
2.8. Synthesis of 2,10-dibromo-5,7-bis(2-ethylhexyl)tetrathieno[2,3-b:3',4'-f:3'',2''-j:2''',3''',4''',5'''-lmn][4,7]phenanthroline	10
2.9. Synthesis of PTPP1-BDT.....	11
3. NMR Spectroscopic Characterization:	12
3.1. Figure S1: ¹ H NMR spectra of precursor 1,3-dibromo-5,7-bis(2-decyltetradecyl)-4H,8H-benzo[1,2-c:4,5-c']dithiophene-4,8-dione.....	12

3.2.	Figure S2: ^{13}C NMR spectra of precursor 1,3-dibromo-5,7-bis(2-decyltetradecyl)-4H,8H-benzo[1,2-c:4,5-c']dithiophene-4,8-dione	13
3.3.	Figure S3: ^1H NMR spectra of precursor tert-butyl (2-bromothiophen-3-yl)carbamate	14
3.4.	Figure S4: ^1H NMR spectra of tert-butyl (2-(trimethylstannyl)thiophen-3-yl)carbamate	15
3.5.	Figure S5: ^1H NMR spectra of di-tert-butyl ((5,7-bis(2-ethylhexyl)-4,8-dioxo-4H,8H-benzo[1,2-c:4,5-c']dithiophene-1,3-diyl)bis(thiophene-2,3-diyl))dicarbamate (3a)	16
3.6.	Figure S6: ^{13}C NMR spectra of di-tert-butyl ((5,7-bis(2-ethylhexyl)-4,8-dioxo-4H,8H-benzo[1,2-c:4,5-c']dithiophene-1,3-diyl)bis(thiophene-2,3-diyl))dicarbamate (3a)	17
3.7.	Figure S7: ^1H NMR spectra of 5,7-bis(2-ethylhexyl)tetrathieno[2,3-b:3',4'-f:3'',2''-j:2''',3''',4''',5'''-lmn][4,7]phenanthroline (TTP1)	18
3.8.	Figure S8: ^{13}C NMR spectra of 5,7-bis(2-ethylhexyl)tetrathieno[2,3-b:3',4'-f:3'',2''-j:2''',3''',4''',5'''-lmn][4,7]phenanthroline (TTP1)	19
3.9.	Figure S9: ^1H NMR spectra of 5,7-bis(2-ethylhexyl)-2,10-bis(trimethylstannyl)tetrathieno[2,3-b:3',4'-f:3'',2''-j:2''',3''',4''',5'''-lmn][4,7]phenanthroline (TTP1-Sn)	20
3.10.	Figure S10: ^{13}C NMR spectra of 5,7-bis(2-ethylhexyl)-2,10-bis(trimethylstannyl)tetrathieno[2,3-b:3',4'-f:3'',2''-j:2''',3''',4''',5'''-lmn][4,7]phenanthroline (TTP1-Sn)	
	21	
3.11.	Figure S11: ^1H NMR spectra of 2-bromo-5,7-bis(2-ethylhexyl)tetrathieno[2,3-b:3',4'-f:3'',2''-j:2''',3''',4''',5'''-lmn][4,7]phenanthroline	22
3.12.	Figure S12: ^{13}C NMR spectra of 2-bromo-5,7-bis(2-ethylhexyl)tetrathieno[2,3-b:3',4'-f:3'',2''-j:2''',3''',4''',5'''-lmn][4,7]phenanthroline	23
3.13.	Figure S13: ^1H NMR spectra of 2,10-dibromo-5,7-bis(2-ethylhexyl)tetrathieno[2,3-b:3',4'-f:3'',2''-j:2''',3''',4''',5'''-lmn][4,7]phenanthroline	24
3.14.	Figure S14: ^1H NMR spectra of di-tert-butyl ((5,7-bis(2-decyltetradecyl)-4,8-dioxo-4H,8H-benzo[1,2-c:4,5-c']dithiophene-1,3-diyl)bis(thiophene-2,3-diyl))dicarbamate (3b).....	25
3.15.	Figure S15: ^{13}C NMR spectra of di-tert-butyl ((5,7-bis(2-decyltetradecyl)-4,8-dioxo-4H,8H-benzo[1,2-c:4,5-c']dithiophene-1,3-diyl)bis(thiophene-2,3-diyl))dicarbamate (3b).....	26
3.16.	Figure S16: ^1H NMR spectra of 5,7-bis(2-decyltetradecyl)tetrathieno[2,3-b:3',4'-f:3'',2''-j:2''',3''',4''',5'''-lmn][4,7]phenanthroline (TTP2)	27
3.17.	Figure S17: ^{13}C NMR spectra of 5,7-bis(2-decyltetradecyl)tetrathieno[2,3-b:3',4'-f:3'',2''-j:2''',3''',4''',5'''-lmn][4,7]phenanthroline (TTP2)	28
3.18.	Figure S18: ^1H NMR spectra of tert-butyl (2-(7,9-bis(2-decyltetradecyl)-6-oxo-6H-trithieno[3,2-b:2',3',4'-de:3'',4''-h]quinolin-5-yl)thiophen-3-yl)carbamate.....	29
3.19.	Figure S19: ^1H NMR spectra of 5,7-bis(2-decyltetradecyl)-2,10-bis(trimethylstannyl)tetrathieno[2,3-b:3',4'-f:3'',2''-j:2''',3''',4''',5'''-lmn][4,7]phenanthroline (TTP2-Sn)	

3.20.	Figure S20: ^{13}C NMR spectra of 5,7-bis(2-decyltetradecyl)-2,10-bis(trimethylstannyl)tetrathieno[2,3-b:3',4'-f:3'',2''-j:2''',3''',4''',5'''-lmn][4,7]phenanthroline (TTP2-Sn)	31
4.	Gel permeation chromatography	32
4.1.	Figure S21: GPC analysis of PTPP-BDT.....	32
	Table S1. Conditions explored for one pot acid catalyzed deprotection and ring fusion	32
5.	Photovoltaic Measurements.....	32
5.1.	Table S2. Optimisation of D/A concentration for PTPP-BDT:Y6 based Organic Solar Cells	32
5.2.	Table S3. Optimisation of D/A ratio for PTPP-BDT:Y6 based Organic Solar Cells.....	33
5.3.	Table S4. Photovoltaic performance of PBDB-T:Y6 BHJ solar cells. Blend concentration was 19.8 mg/mL with D/A ratio of 1:1.2.....	34
5.4.	Figure S22. External Quantum Efficiency spectra of fabricated Organic Solar Cells with different D/A concentration and D/A ratio.	34
5.5.	Figure S23. Fitting of double logarithmic dark J-V curve of PTPP-BDT based hole only devices. Hole mobility was measured by considering Trap-free region where the slope of curve was 2.....	35
5.6.	Figure S24. Photovoltaic characterisation of devices based on novel PTPP-BDT1:Y6 vs reference PBDB-T:Y6 over time. Values are normalised. (a) Power conversion efficiency (b) Open circuit voltage (c) Short circuit current (d) Fill Factor of fabricated devices.....	35

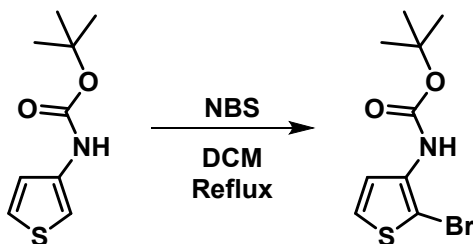
1. Materials and characterization

All commercially available solvents were distilled and freshly dried by standard drying methods. Reagents and chemicals were used as received without further purification unless otherwise stated. (1) was prepared according to reported procedure, Monomers (2) were purchased from Solarmer inc. Unless otherwise stated, all operations and reactions were carried out under argon using standard Schlenk line techniques. Analytical thin-layer chromatography was performed on Merck aluminum-backed plates pre-coated with silica (0.2 mm, 60 F254) gel. Plates were visualized by exposure to UV light (254 nm) or (365 nm). ^1H and ^{13}C NMR spectra were recorded on a Bruker AV-400 (400 MHz or 600 MHz), using the residual solvent resonance of CDCl_3 or TMS as an internal reference and are given in ppm. mass spectra were recorded on Triple Quad LC/MS 6420 (Agilent Technologies) spectrometer. Number-average (M_n) and weight average (M_w) were determined by Agilent Technologies 1200 series GPC running in chlorobenzene

at 80 °C, using two PL mixed B columns in series, and calibrated against narrow polydispersity polystyrene standards. UV-vis spectra were recorded on a PerkinElmer Lambda 1050 UV-Vis spectrometer. Differential scanning calorimetry (DSC) analysis were recorded on PerkinElmer Jade DSC Differential Scanning Calorimeter under nitrogen at 5 °C min⁻¹ of heating rate from 30 °C to 350 °C in two cycles heating-cooling, and thermogravimetric analysis (TGA) curves were collected on Mettler in nitrogen at 10 °C min⁻¹ of heating rate from 30 °C to 600 °C. Cyclic voltammetry (CV) measurements of polymers films were performed under argon atmosphere using a CHI760E Voltammetry analyzer with 0.1 M tetra-n-butylammonium hexafluorophosphate in acetonitrile as the supporting electrolyte. A glassy carbon working electrode, a platinum wire counter electrode, and a silver wire (Ag/AgNO₃) reference electrode were employed, and the ferrocene/ferrocenium (Fc/Fc⁺) was used as the internal reference for all measurements. The scanning rate was 100 mV/s. Polymer films were drop-casted from chloroform solutions on a glassy carbon working electrode (2 mm in diameter). A Bruker Dimension Icon Atomic Force Microscopy (AFM) with Nanoscope V controller was used to collect height and phase images of the samples. The images were collected at 2×2 μm area using the tapping method and a Bruker Tespa V2 probe.

2. Synthetic Procedures :

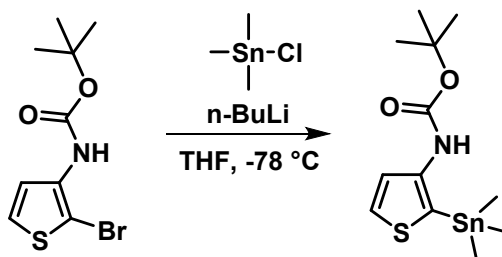
2.1. Synthesis of tert-butyl (2-bromothiophen-3-yl)carbamate



To a boiling solution of tert-butyl thiophen-3-ylcarbamate (5.5 g, 27.6 mmol) in dichloromethane (250 mL) was added portion wise recrystallized N-Bromosuccinamide (5.16 g, 28.98 mmol) with rigorous stirring. Following the addition, the bath temperature was raised to 65 °C and maintained for 30 min and then

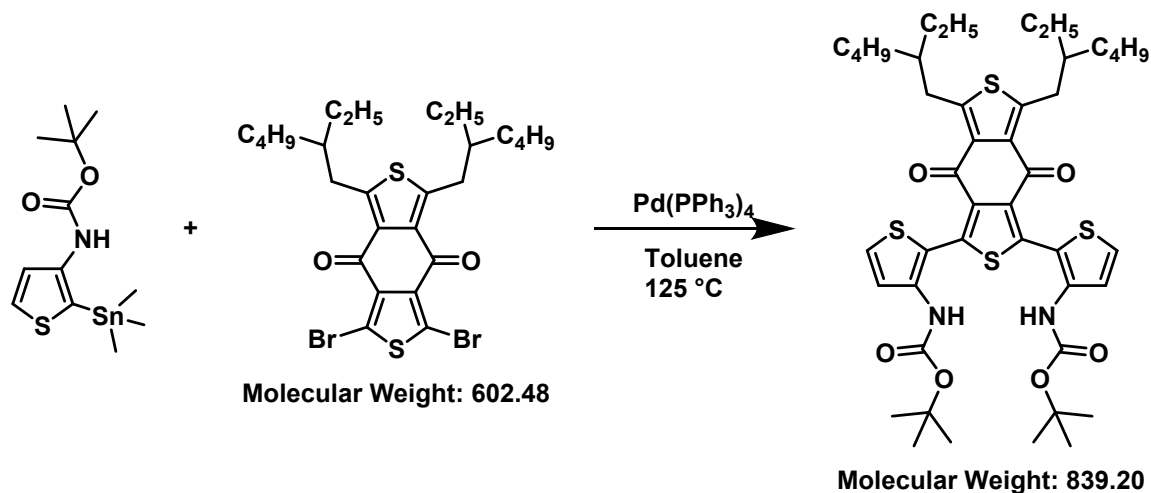
allowed to cool to room temperature. The reaction mixture was washed with water, brine, dried over anhydrous MgSO_4 , filtered and then concentrated to obtain a viscous oil. A short column chromatography over silica (10% EtOAc: Hexane) provided clear oil of tert-butyl (2-bromothiophen-3-yl)carbamate (7.45 g, 97 %) which crystallized on standing. ^1H NMR (400 MHz, CDCl_3) 7.55 (s, 1H), 7.23 (d, $J = 5.9$ Hz, 1H), 6.57 (s, 1H), 1.44 (s, 9H). ^{13}C NMR (100 MHz, CDCl_3) δ 152.15, 135.74, 124.80, 121.68, 94.10, 81.14, 28.28. FTMS (APCI, m/z of $[\text{MH}^+]$): Calcd. For $[\text{C}_9\text{H}_{12}\text{BrNO}_2\text{S} + \text{H}]^+$, $m/z = 276.9772$. Found: $m/z = 277.98$ $[\text{M}+\text{H}]^+$.

2.2. Synthesis of tert-butyl (2-(trimethylstannyl)thiophen-3-yl)carbamate



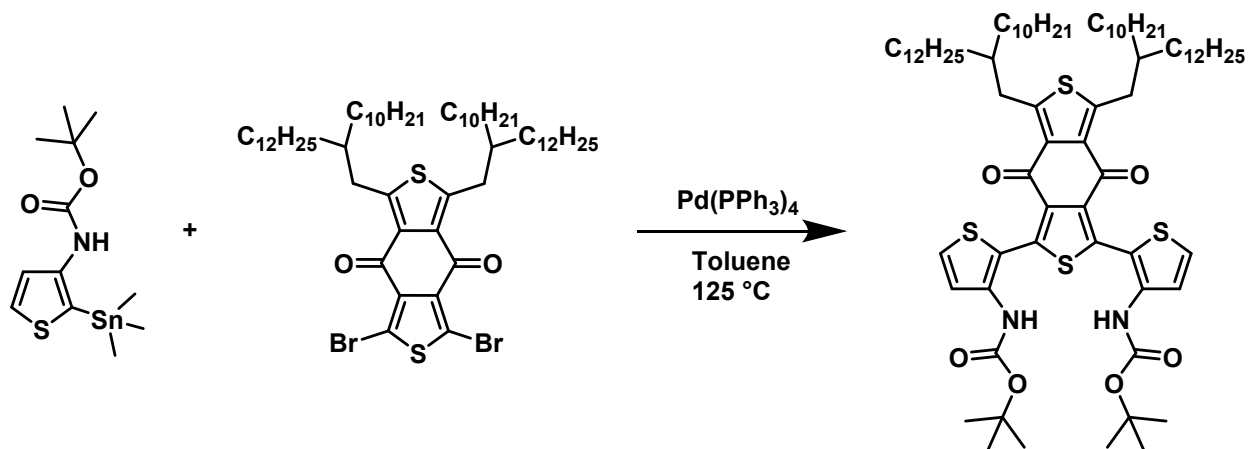
To a solution of tert-butyl (2-bromothiophen-3-yl)carbamate (6.5g, 23.36 mmol) in freshly prepared anhydrous THF (70 mL) at $-78\text{ }^\circ\text{C}$ was added dropwise a 2.5 M solution of n-Butyl Lithium (21.03 mL, 52.57 mmol). The reaction mixture was further stirred for 1.5h followed by addition of 1M solution of chlorotrimethyl stannane (25.72 mL, 25.7 mmol) in Hexanes. After stirring for further 15 min at $-78\text{ }^\circ\text{C}$ the reaction mixture was allowed to warm to room temperature and then quenched with saturated ammonium chloride 50 ml. The reaction mixture was diluted with diethyl ether and washed with water, brine, dried over anhydrous MgSO_4 , filtered and then concentrated to obtain tert-butyl (2-(trimethylstannyl)thiophen-3-yl)carbamate (8.31 g, 98.2 %) ^1H NMR (400 MHz, CDCl_3) δ 7.45 (d, $J = 4.8$ Hz, 1H), 7.09 (d, $J = 4.8$ Hz, 1H), 6.34 (s, 1H), 1.46 (s, 9H), 0.32 (s, 9H). FTMS (APCI, m/z of $[\text{MH}^+]$): Calcd. for $[\text{C}_{12}\text{H}_{21}\text{NO}_2\text{SSn} + \text{H}]^+$, $m/z = 363.0315$. Found: $m/z = 364.11$ $[\text{M}+\text{H}]^+$.

2.3. Synthesis of di-tert-butyl ((5,7-bis(2-ethylhexyl)-4,8-dioxo-4H,8H-benzo[1,2-c:4,5-c']dithiophene-1,3-diyl)bis(thiophene-2,3-diyl))dicarbamate



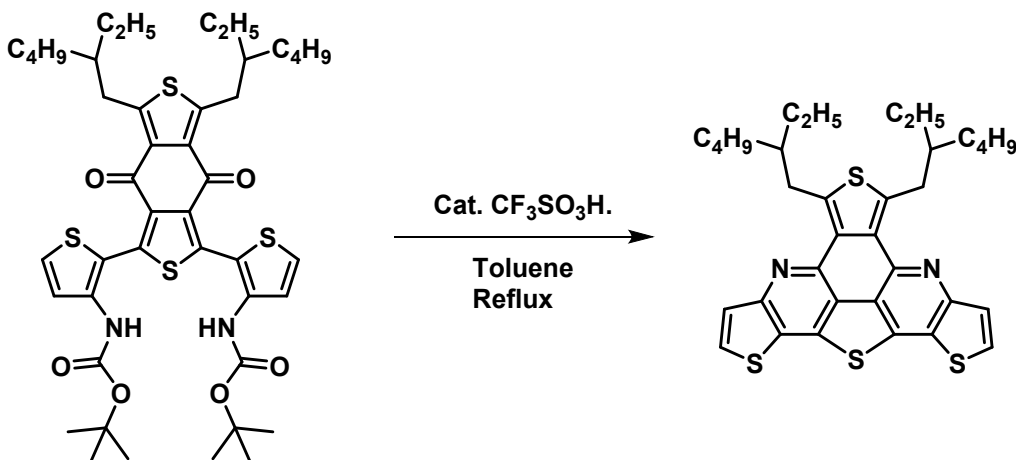
Toluene (9 mL) was added to a deoxygenated mixture of 1,3-dibromo-5,7-bis(2-ethylhexyl)-4H,8H-benzo[1,2-c:4,5-c']dithiophene-4,8-dione (1.2 g, 1.99 mmol), tert-butyl (2-(trimethylstannyl)thiophen-3-yl)carbamate (1.58 g, 4.38 mmol) and Tetrakis(triphenylphosphine)-palladium(0) (115 mg, 0.099mmol) in a sealed microwave vial. The mixture was further purged with argon for 30 min, and then stirred at 120 °C for overnight. The reaction mixture was cooled to room temperature filtered through celite layered on top with silica bed, eluted with chloroform and concentrated to obtain dark green-brown viscous oil. Column chromatography over silica (30% CHCl₃:Hexane) provided di-tert-butyl ((5,7-bis(2-ethylhexyl)-4,8-dioxo-4H,8H-benzo[1,2-c:4,5-c']dithiophene-1,3-diyl)bis(thiophene-2,3-diyl))dicarbamate (1.2g, 71%) as clear yellow viscous oil. ¹H NMR (400 MHz, CDCl₃) δ 7.63 (s, 2H), 7.41 (d, J = 5.5 Hz, 4H), 3.47 – 3.11 (m, 4H), 1.87 – 1.69 (m, 2H), 1.49 (s, 18H), 1.43 – 1.19 (m, 16H), 0.90 (m, 12H). ¹³C NMR (100 MHz, CDCl₃) δ 179.05, 155.03, 153.19, 142.45, 137.64, 134.33, 133.04, 127.20, 125.08, 116.28, 80.56, 41.19, 41.16, 33.84, 32.87, 28.83, 28.31, 25.98, 23.02, 14.10, 10.82. FTMS (APCI, m/z of [MH⁺]): Calcd. for [C₄₄H₅₈N₂O₆S₄ + H]⁺, m/z = 838.3178. Found: m/z = 839.21 [M+H]⁺.

2.4. Synthesis of di-tert-butyl ((5,7-bis(2-decyltetradecyl)-4,8-dioxo-4H,8H-benzo[1,2-c:4,5-c']dithiophene-1,3-diyl)bis(thiophene-2,3-diyl))dicarbamate



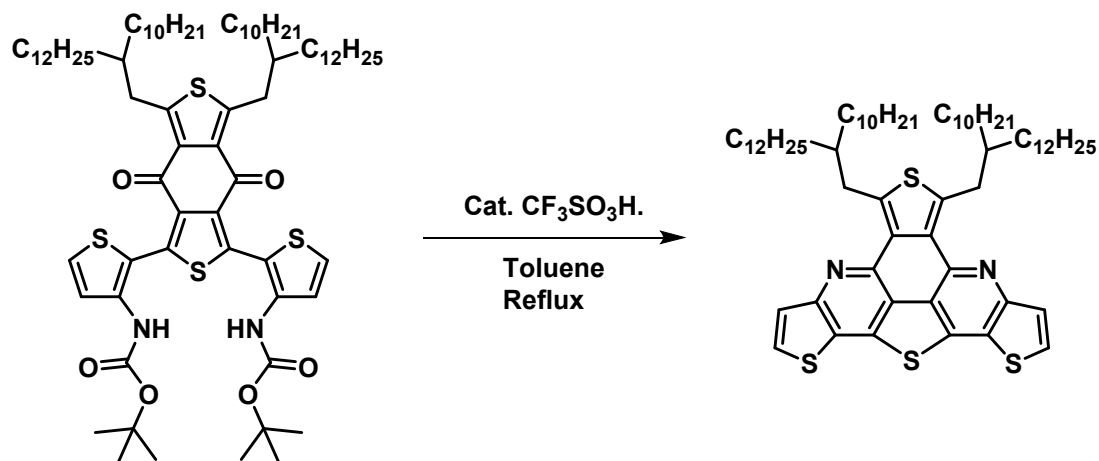
Using the above procedure and column chromatography over silica (25% DCM:Hexane) was obtained (1g, 85%) as clear yellow viscous oil. ^1H NMR (400 MHz, CDCl_3) δ 7.62 (s, 2H), 7.41 (d, $J = 6.5$ Hz, 4H), 3.27 (d, $J = 7.0$ Hz, 4H), 1.83 (s, 2H), 1.49 (s, 18H), 1.42 – 1.11 (m, 80H), 0.88 (m, 12H). ^{13}C NMR (100 MHz, CDCl_3) δ 179.01, 154.78, 153.14, 142.51, 137.72, 134.30, 133.07, 127.18, 125.12, 116.30, 80.42, 39.65, 34.37, 33.83, 31.99, 30.08, 29.74, 29.43, 28.34, 26.64, 22.75, 14.17. FTMS (APCI, m/z of $[\text{MH}^+]$): Calcd. for $[\text{C}_{76}\text{H}_{122}\text{N}_2\text{O}_6\text{S}_4 + \text{H}]^+$, $m/z = 1286.8186$. Found: $m/z = 1287.83$ $[\text{M}+\text{H}]^+$.

2.5. Synthesis of 5,7-bis(2-ethylhexyl)tetrathieno[2,3-b:3',4'-f:3'',2''-j:2''',3''',4''',5'''-lmn][4,7]phenanthroline



To a solution of di-tert-butyl ((5,7-bis(2-ethylhexyl)-4,8-dioxo-4H,8H-benzo[1,2-c:4,5-c']dithiophene-1,3-diyl)bis(thiophene-2,3-diyl)dicarbamate (1g, 1.191 mmol) in anhydrous toluene (50 mL) was added trifluoromethanesulfonic acid (2 mL) and refluxed for 48h. The reaction mixture was concentrated over rotary, dissolved in dichloromethane (50mL), washed with water, dried over anhydrous MgSO_4 and concentrated to obtain crude solid. Column chromatography over silica gel (20% CHCl_3 : Hexane) provided 5,7-bis(2-ethylhexyl)tetrathieno[2,3-b:3',4'-f:3'',2''-j:2''',3''',4''',5'''-lmn][4,7]phenanthroline as yellow solid (672 mg, 93 %). ^1H NMR (400 MHz, CDCl_3) δ 7.56 (d, J = 5.4 Hz, 2H), 7.50 (d, J = 5.4 Hz, 2H), 3.63 – 3.36 (m, 4H), 2.03 – 1.82 (m, 2H), 1.51 – 1.17 (m, 16H), 1.05 – 0.75 (m, 12H). ^{13}C NMR (100 MHz, CDCl_3) δ 154.60, 145.04, 141.37, 141.34, 138.04, 131.68, 127.45, 126.10, 123.35, 123.20, 77.36, 77.04, 76.73, 40.40, 40.36, 33.89, 32.84, 32.80, 31.63, 28.91, 28.89, 25.96, 23.30, 22.69, 14.27, 14.16, 10.95, 10.92. FTMS (APCI, m/z of $[\text{MH}^+]$): Calcd. for $[\text{C}_{34}\text{H}_{38}\text{N}_2\text{S}_4 + \text{H}]^+$, m/z = 602.1918. Found: m/z = 603.21 $[\text{M}+\text{H}]^+$.

2.6. Synthesis of 5,7-bis(2-decyltetradecyl)tetrathieno[2,3-b:3',4'-f:3'',2''-j:2''',3''',4''',5'''-lmn][4,7]phenanthroline

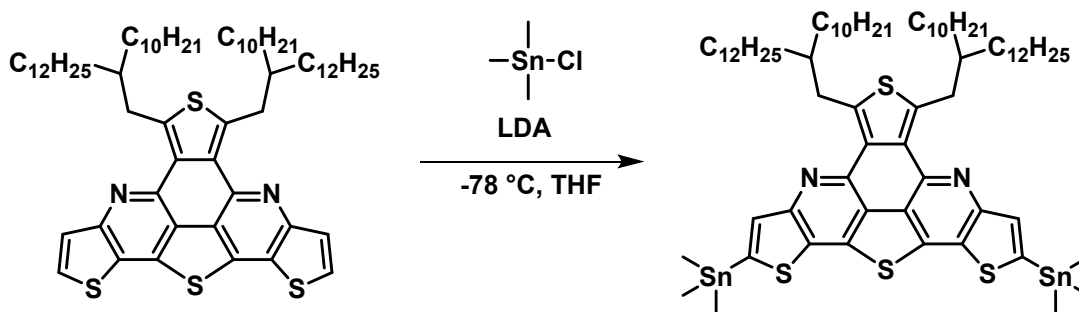


^1H NMR (400 MHz, CDCl_3) δ 7.73 (d, J = 5.4 Hz, 2H), 7.70 (d, J = 5.4 Hz, 2H), 3.70 (d, J = 7.1 Hz, 4H), 2.06 (s, 2H), 1.51 – 1.33 (m, 16H), 1.22 (m, 64H), 0.86 (m, 12H). ^{13}C NMR (100 MHz, CDCl_3) δ 154.92, 145.49, 141.82, 138.48, 131.86, 127.76, 126.38, 123.83, 123.54, 39.32, 34.40, 33.63, 31.95, 30.25, 29.75, 29.70,

29.39, 26.59, 22.71, 14.13. FTMS (APCI, m/z of $[MH^+]$): Calcd. for $[C_{66}H_{102}N_2S_4 + H]^+$, $m/z = 1050.6926$.

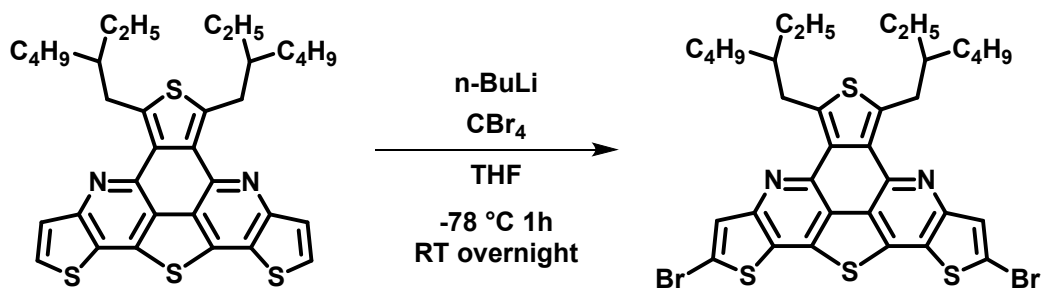
Found: $m/z = 1051.73 [M+H]^+$.

2.7. Synthesis of 5,7-bis(2-decyltetradecyl)-2,10-bis(trimethylstannyl)tetrathieno[2,3-b:3',4'-f:3'',2''-j:2''',3''',4''',5'''-lmn][4,7]phenanthroline



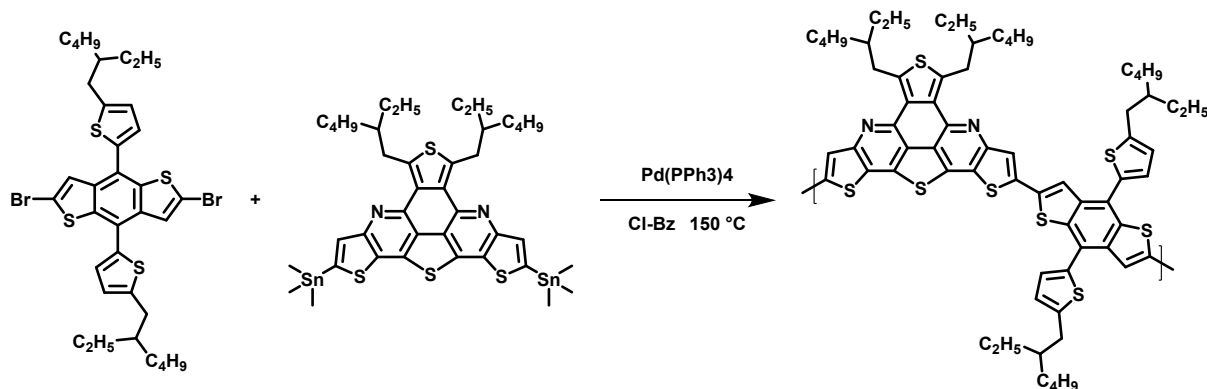
To a solution of 5,7-bis(2-decyltetradecyl)tetrathieno[2,3-b:3',4'-f:3'',2''-j:2''',3''',4''',5'''-lmn][4,7]phenanthroline (170.1 mg, 0.161 mmol) in a freshly prepared anhydrous THF (3 mL) at $-78\text{ }^{\circ}\text{C}$ was added dropwise a 2M solution of Lithium diisopropyl amide (0.245 mL, 0.485 mmol). The reaction mixture was further stirred for 2 h followed by addition of 1M solution of chlorotrimethyl stannane (0.405 mL, 0.404 mmol) in Hexanes. After stirring for further 15 min at $-78\text{ }^{\circ}\text{C}$ the reaction mixture was allowed to warm to room temperature and then quenched with saturated ammonium chloride 5 ml. The reaction mixture was diluted with diethyl ether and washed with water, brine, dried over anhydrous MgSO_4 , filtered and then concentrated to obtain 5,7-bis(2-decyltetradecyl)-2,10-bis(trimethylstannyl)tetrathieno[2,3-b:3',4'-f:3'',2''-j:2''',3''',4''',5'''-lmn][4,7]phenanthroline (0.217 g, 97.4 %) ^1H NMR (400 MHz, CDCl_3) δ 7.87 (s, 2H), 3.84–3.82 (m, 4H), 2.12 (s, 2H), 1.46 (d, $J = 4.1$ Hz, 16H), 1.31 – 0.97 (m, 64H), 0.86 (m, 12H), 0.53 (s, 18H). ^{13}C NMR (100 MHz, CDCl_3) δ 156.53, 145.60, 142.76, 141.71, 138.24, 134.23, 132.33, 128.26, 128.00, 123.55, 39.59, 34.44, 33.76, 31.94, 31.59, 30.28, 29.81, 29.77, 29.72, 29.68, 29.38, 29.36, 26.75, 22.69, 14.11, -8.22. FTMS (APCI, m/z of $[MH^+]$): Calcd. for $[C_{72}H_{118}N_2S_4Sn_2 + H]^+$, $m/z = 1378.6222$. Found: $m/z = 1379.65 [M+H]^+$.

2.8. Synthesis of 2,10-dibromo-5,7-bis(2-ethylhexyl)tetrathieno[2,3-b:3',4'-f:3'',2''-j:2''',3''',4''',5'''-lmn][4,7]phenanthroline



To a solution of 5,7-bis(2-ethylhexyl)tetrathieno[2,3-b:3',4'-f:3'',2''-j:2''',3''',4''',5'''-lmn][4,7]phenanthroline (115.1 mg, 0.19 mmol) in a freshly prepared anhydrous THF (3 mL) at -78 °C was added dropwise a 2.5 M solution of n-Butyl lithium (0.230 mL, 0.57 mmol). The reaction mixture was further stirred for 2 h at -78 °C and a solution of tetrabromomethane (158 mg, 0.404 mmol) in 2 ml anhydrous THF was added dropwise. After stirring for further 30 min the reaction mixture was allowed to slowly warm to room temperature for overnight and then diluted with diethyl ether. The precipitate formed was filtered and filtrate was washed with water, brine, dried over anhydrous MgSO₄, filtered and then concentrated. Column chromatography over silica afforded 2,10-dibromo-5,7-bis(2-ethylhexyl)tetrathieno[2,3-b:3',4'-f:3'',2''-j:2''',3''',4''',5'''-lmn][4,7]phenanthroline (0.11 g, 75.8 %), Mono brominated product 2-bromo-5,7-bis(2-ethylhexyl)tetrathieno[2,3-b:3',4'-f:3'',2''-j:2''',3''',4''',5'''-lmn][4,7]phenanthroline was also isolated in ~5 % yield .

2.9. Synthesis of PTPP1-BDT

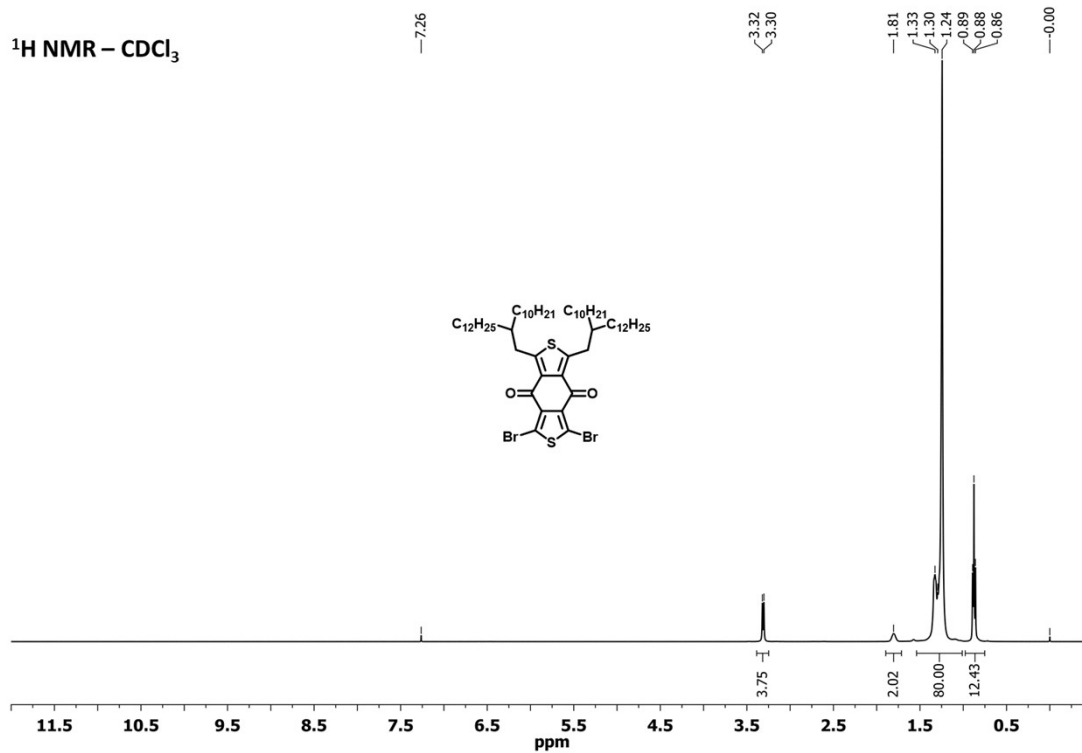


A mixture 2,6-dibromo-4,8-bis(5-(2-ethylhexyl)thiophen-2-yl)benzo[1,2-b:4,5-b']dithiophene (83.2 mg, 0.107 mmol), 5,7-bis(2-ethylhexyl)-2,10-bis(trimethylstannyl)tetrathieno[2,3-b:3',4'-f:3'',2''-j:2''',3''',4''',5'''-lmn][4,7]phenanthroline (100 mg, 0.107 mmol) and Tetrakis(triphenylphosphine)-palladium(0) (3.7 mg, 3 mol %), in microwave vial was sealed and the headspace was replaced with argon.

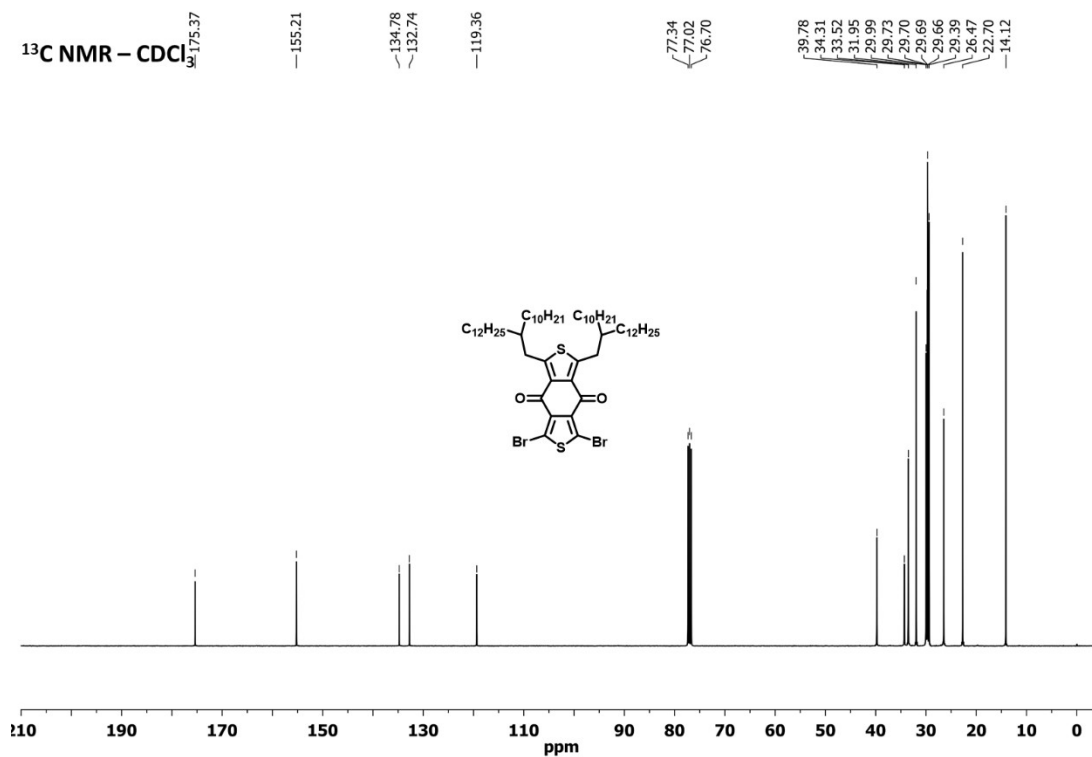
Chlorobenzene (2.5 mL) was injected and reaction mixture was deoxygenated by purging argon for 30 min. After heating the reaction mixture at 150 °C for 5h chlorobenzene 5 mL was injected followed by precipitation in acidic methanol (400 mL) to obtain red colored polymer. Sequential Soxhlet purification with Methanol, Acetone, Hexane and Chloroform was carried out to remove impurities and oligomers. Precipitation of concentrated chlorobenzene fraction in methanol provided pure polymer.

3. NMR Spectroscopic Characterization:

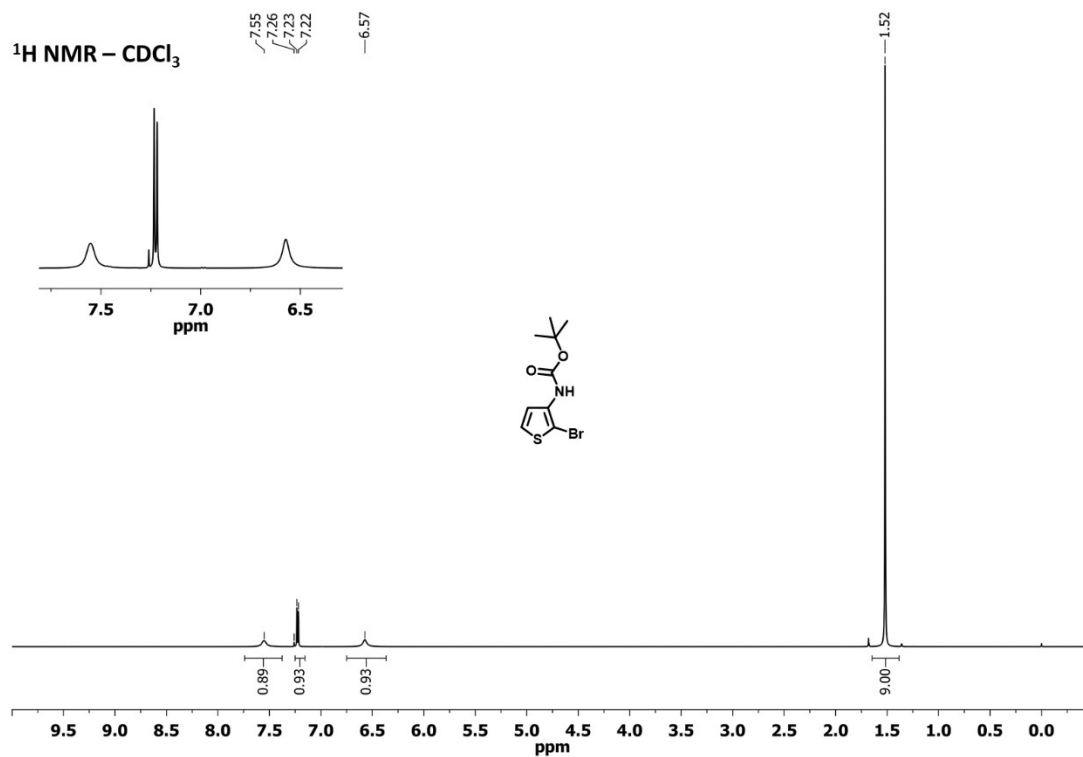
3.1. Figure S1: ^1H NMR spectra of precursor 1,3-dibromo-5,7-bis(2-decyltetradecyl)-4H,8H-benzo[1,2-c:4,5-c']dithiophene-4,8-dione



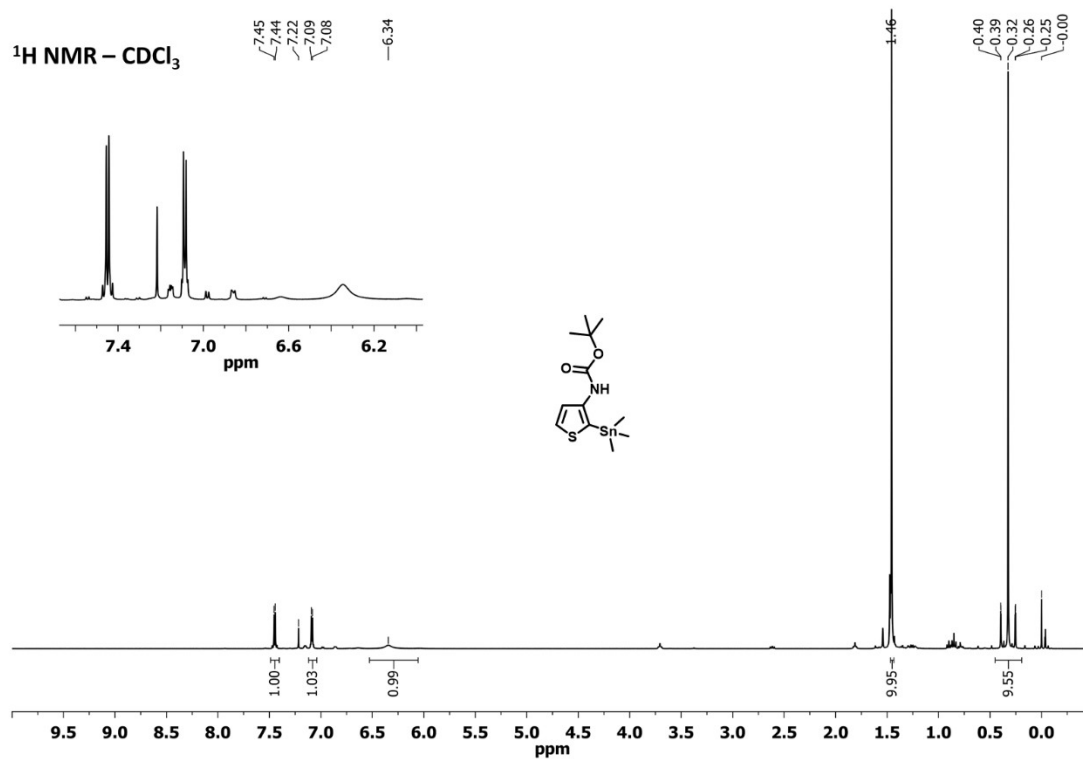
3.2. Figure S2: ^{13}C NMR spectra of precursor 1,3-dibromo-5,7-bis(2-decyltetradecyl)-4H,8H-benzo[1,2-c:4,5-c']dithiophene-4,8-dione



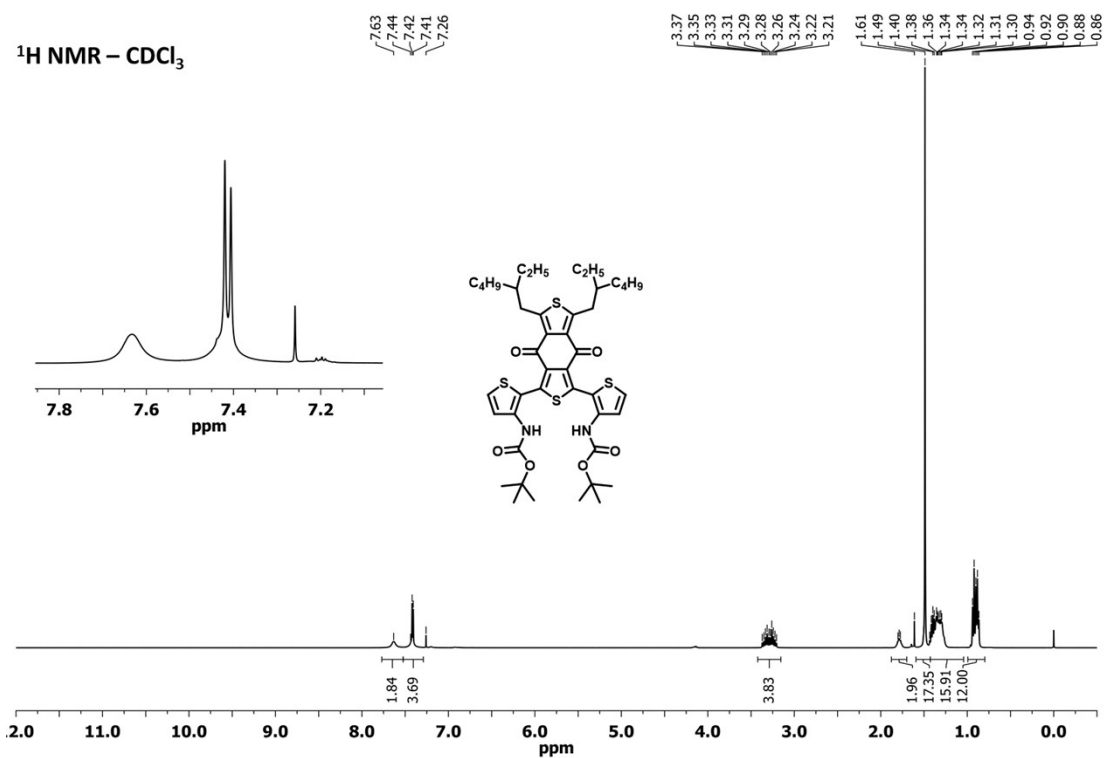
3.3. Figure S3: ^1H NMR spectra of precursor tert-butyl (2-bromothiophen-3-yl)carbamate



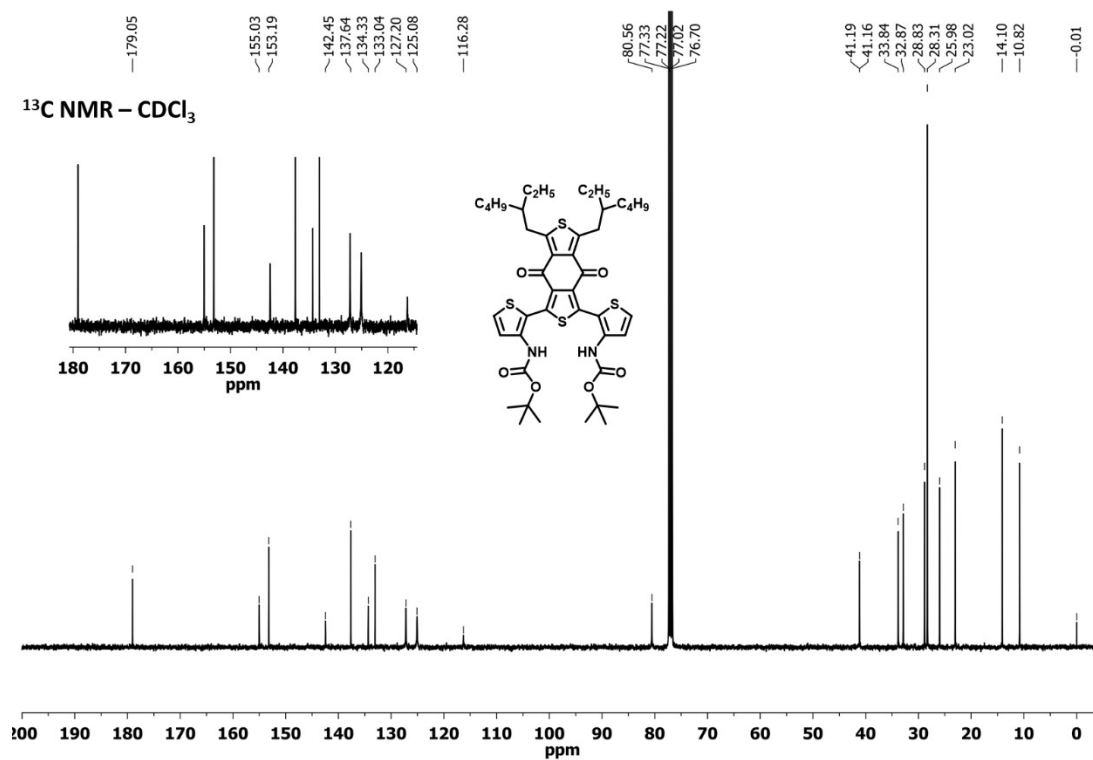
3.4. Figure S4: ^1H NMR spectra of tert-butyl (2-(trimethylstannyl)thiophen-3-yl)carbamate



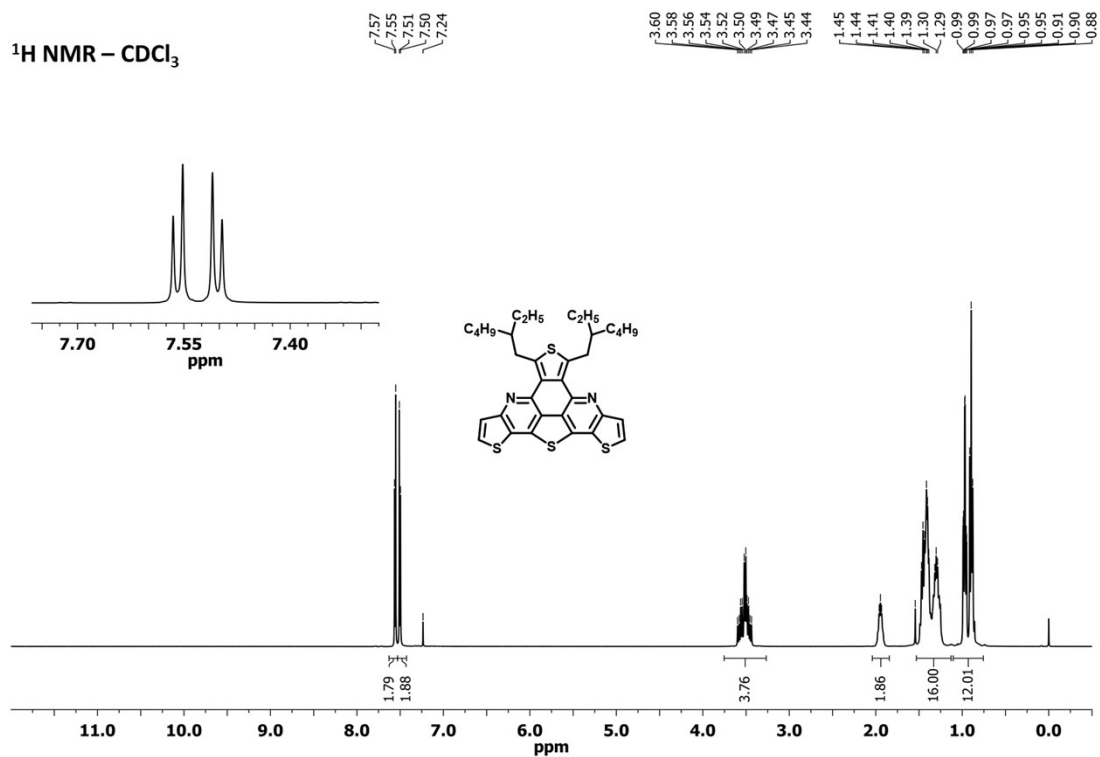
3.5. **Figure S5:** ^1H NMR spectra of di-tert-butyl ((5,7-bis(2-ethylhexyl)-4,8-dioxo-4H,8H-benzo[1,2-c:4,5-c']dithiophene-1,3-diyl)bis(thiophene-2,3-diyl))dicarbamate (3a)



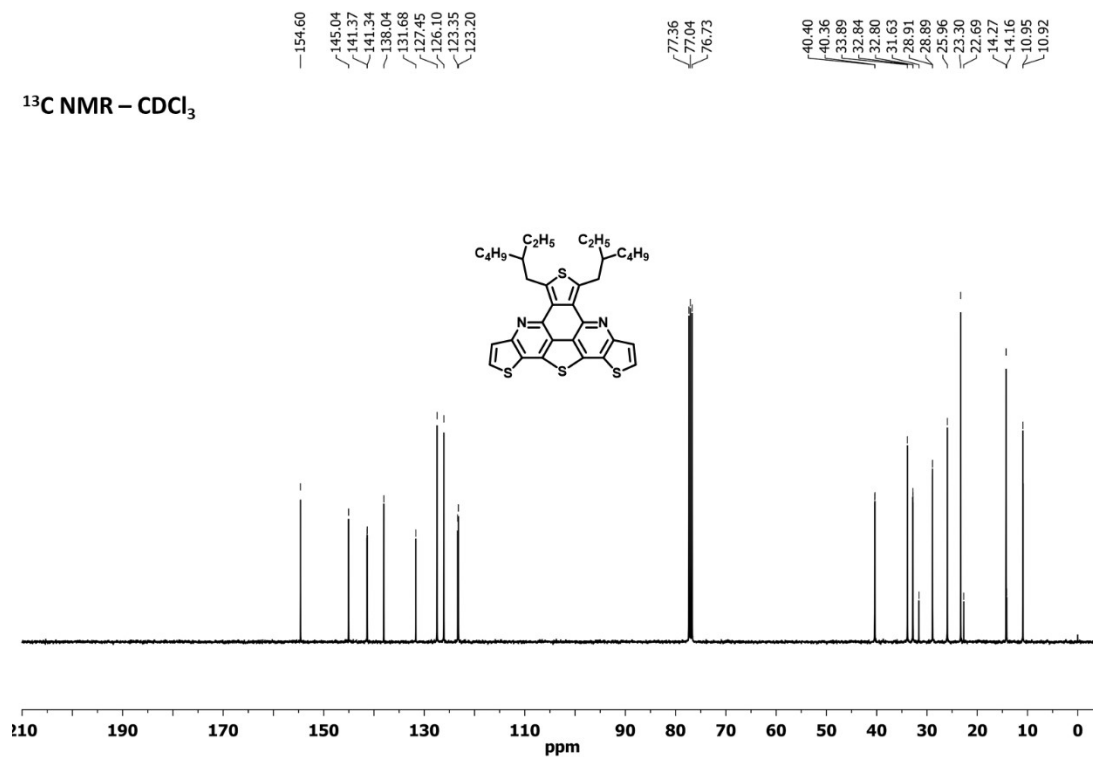
3.6. **Figure S6:** ^{13}C NMR spectra of di-tert-butyl ((5,7-bis(2-ethylhexyl)-4,8-dioxo-4H,8H-benzo[1,2-c:4,5-c']dithiophene-1,3-diyl)bis(thiophene-2,3-diyl))dicarbamate (3a)



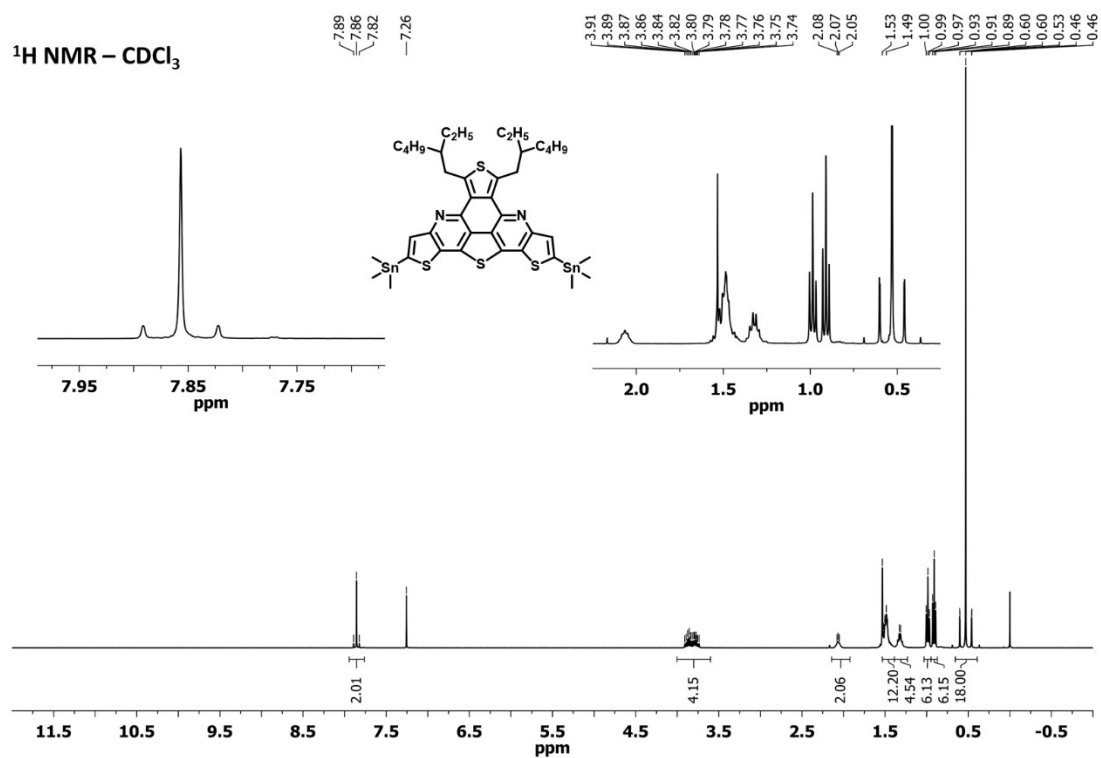
3.7. **Figure S7:** ^1H NMR spectra of 5,7-bis(2-ethylhexyl)tetrathieno[2,3-b:3',4'-f:3'',2''-j:2''',3''',4''',5'''-lmn][4,7]phenanthroline (TTP1)



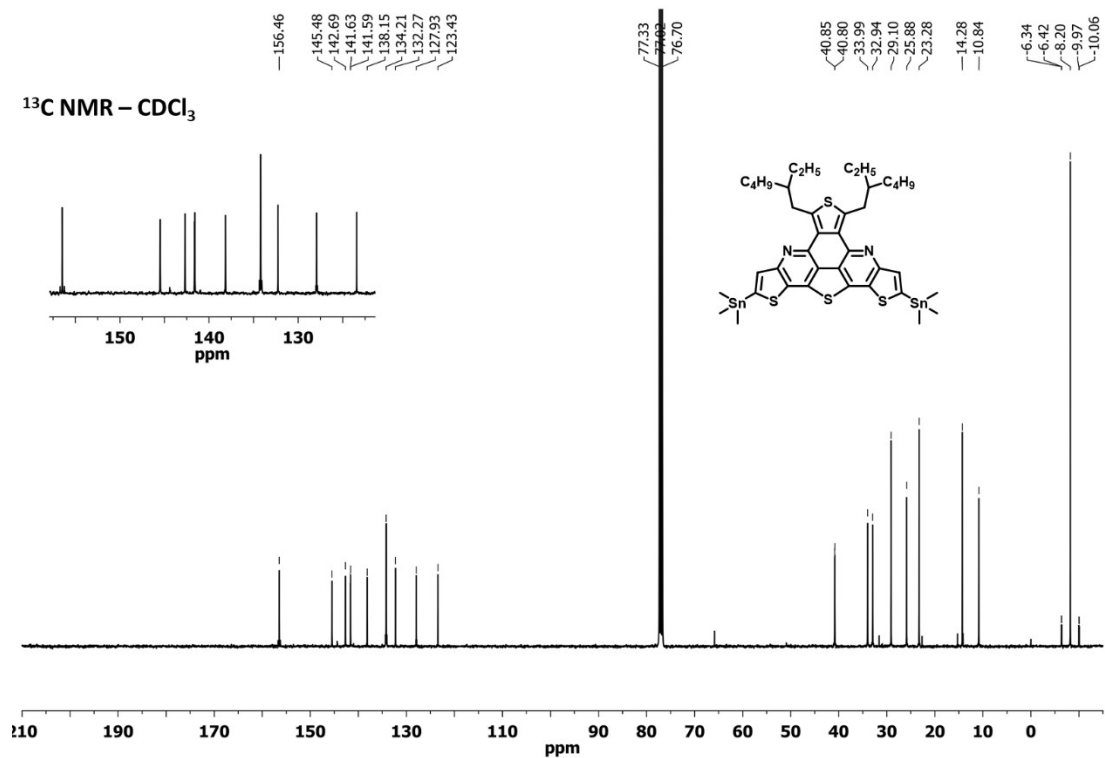
3.8. **Figure S8:** ^{13}C NMR spectra of 5,7-bis(2-ethylhexyl)tetrathieno[2,3-b:3',4'-f:3'',2''-j:2''',3''',4''',5'''-lmn][4,7]phenanthroline (TTP1)



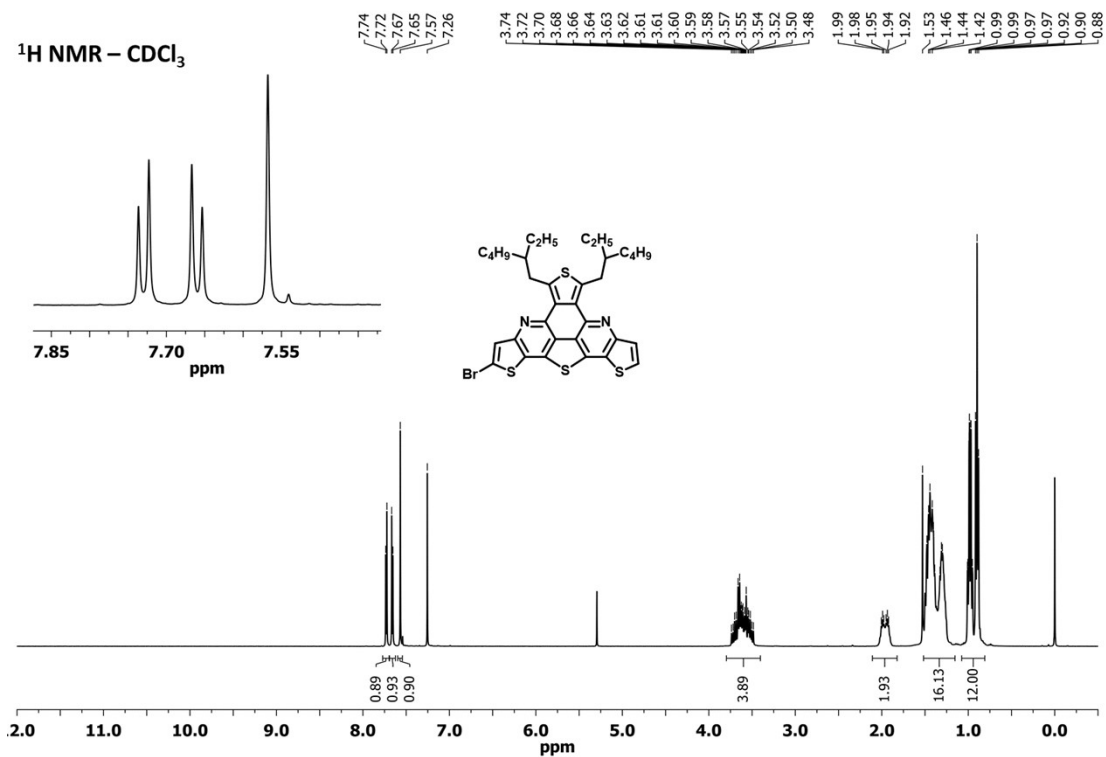
3.9. **Figure S9:** ^1H NMR spectra of 5,7-bis(2-ethylhexyl)-2,10-bis(trimethylstannyl)tetrathieno[2,3-b:3',4'-f:3'',2''-j:2''',3''',4''',5'''-lmn][4,7]phenanthroline (TTP1-Sn)



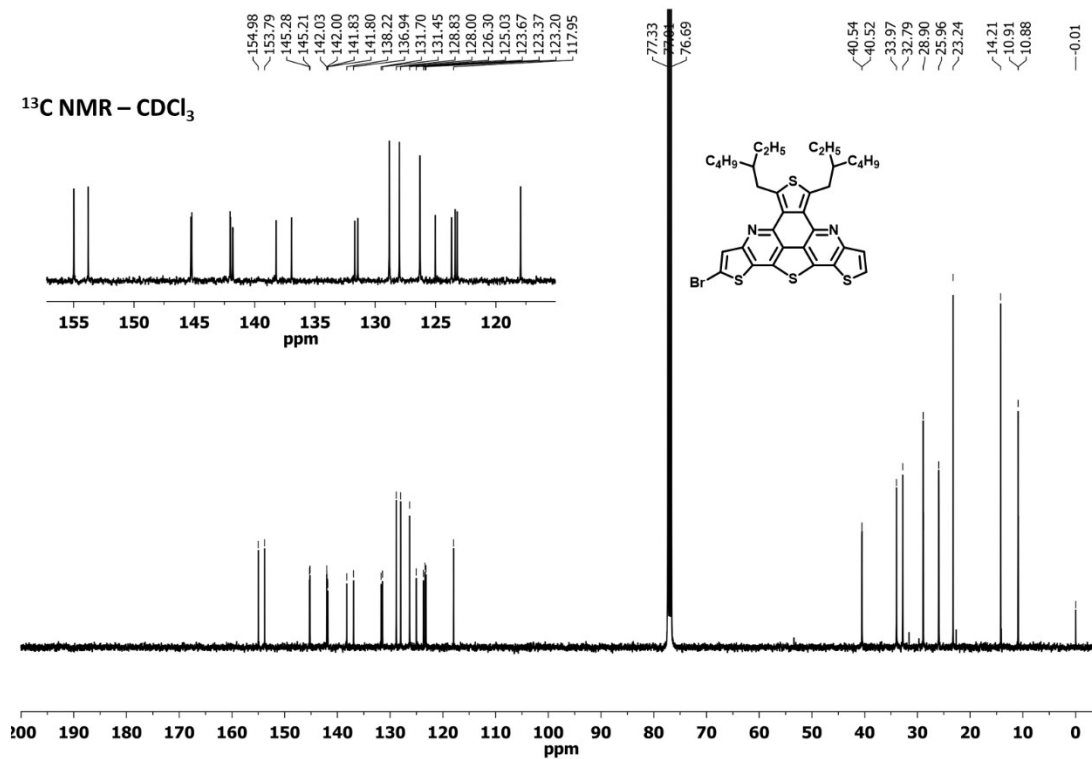
3.10. **Figure S10:** ^{13}C NMR spectra of 5,7-bis(2-ethylhexyl)-2,10-bis(trimethylstannyl)tetrathieno[2,3-b:3',4'-f:3'',2''-j:2''',3''',4''',5'''-lmn][4,7]phenanthroline (TTP1-Sn)



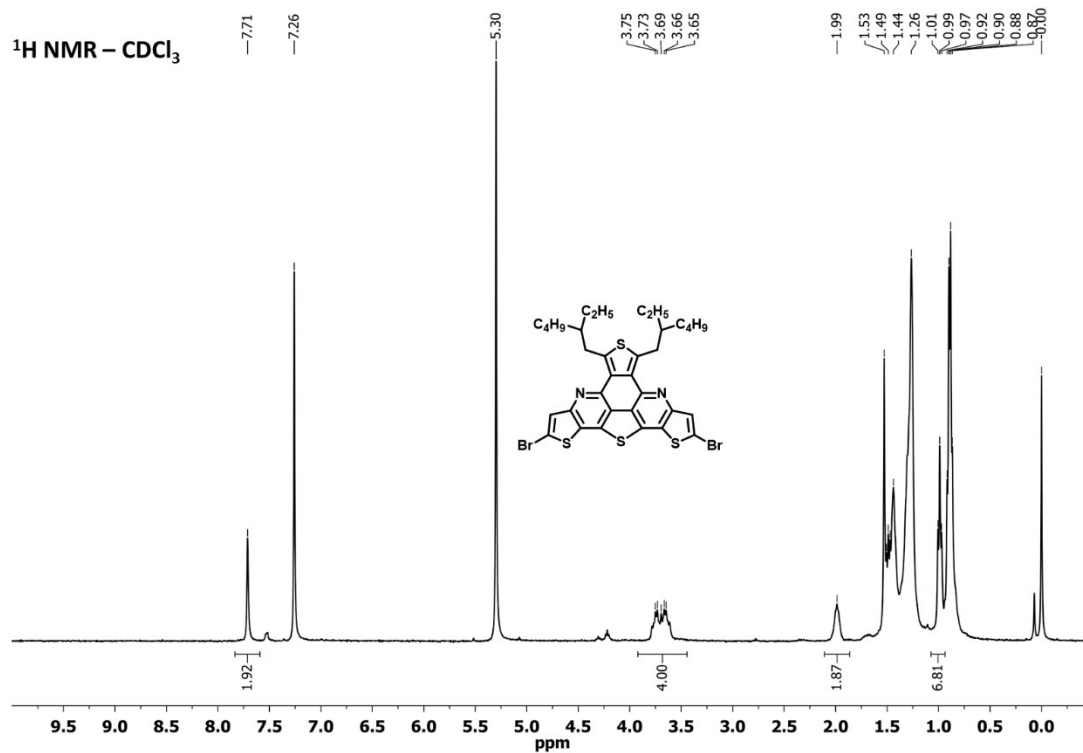
3.11. **Figure S11:** ^1H NMR spectra of 2-bromo-5,7-bis(2-ethylhexyl)tetrathieno[2,3-b:3',4'-f:3'',2''-j:2''',3''',4''',5'''-lmn][4,7]phenanthroline



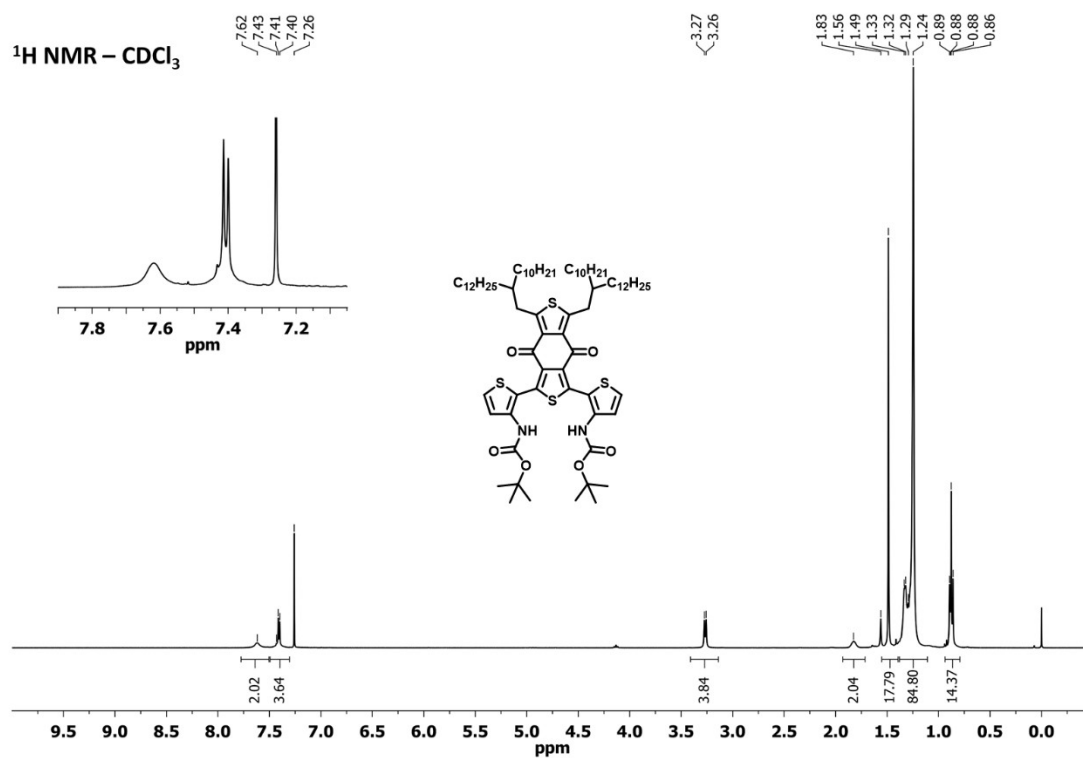
3.12. **Figure S12:** ^{13}C NMR spectra of 2-bromo-5,7-bis(2-ethylhexyl)tetrathieno[2,3-b:3',4'-f:3'',2''-j:2''',3''',4''',5'''-lmn][4,7]phenanthroline



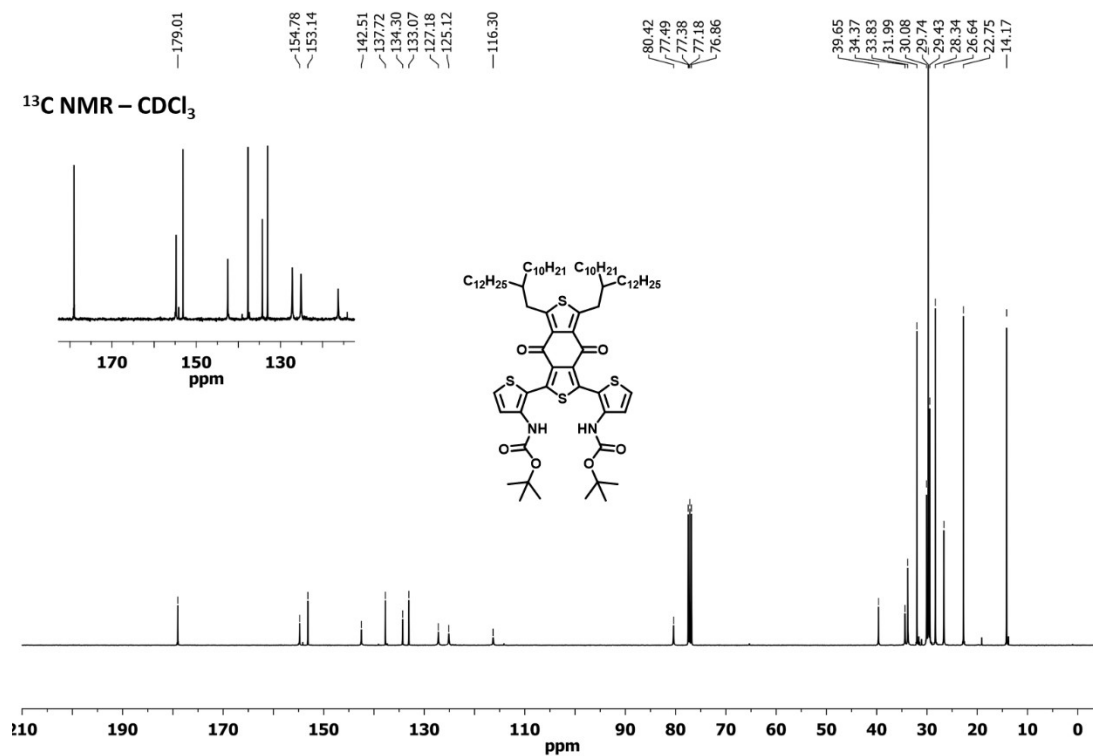
3.13. **Figure S13:** ^1H NMR spectra of 2,10-dibromo-5,7-bis(2-ethylhexyl)tetrathieno[2,3-b:3',4'-f:3'',2''-j:2''',3''',4''',5'''-lmn][4,7]phenanthroline



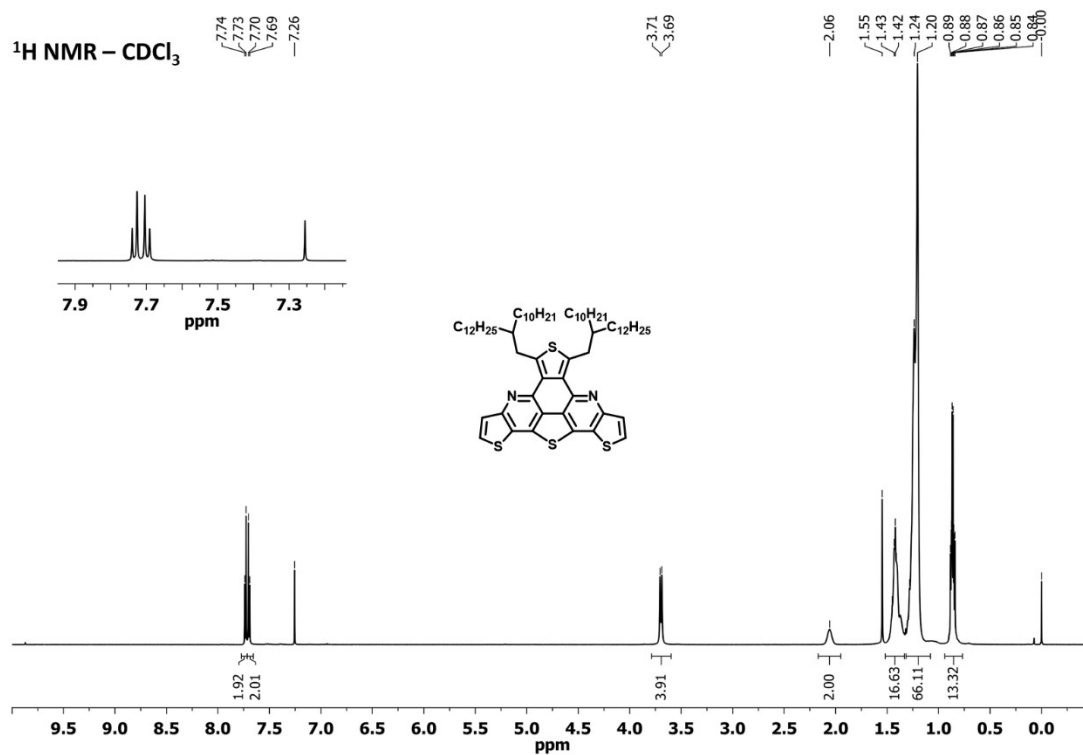
3.14. **Figure S14:** ^1H NMR spectra of di-tert-butyl ((5,7-bis(2-decyltetradecyl)-4,8-dioxo-4H,8H-benzo[1,2-c:4,5-c']dithiophene-1,3-diyl)bis(thiophene-2,3-diyl))dicarbamate (3b)



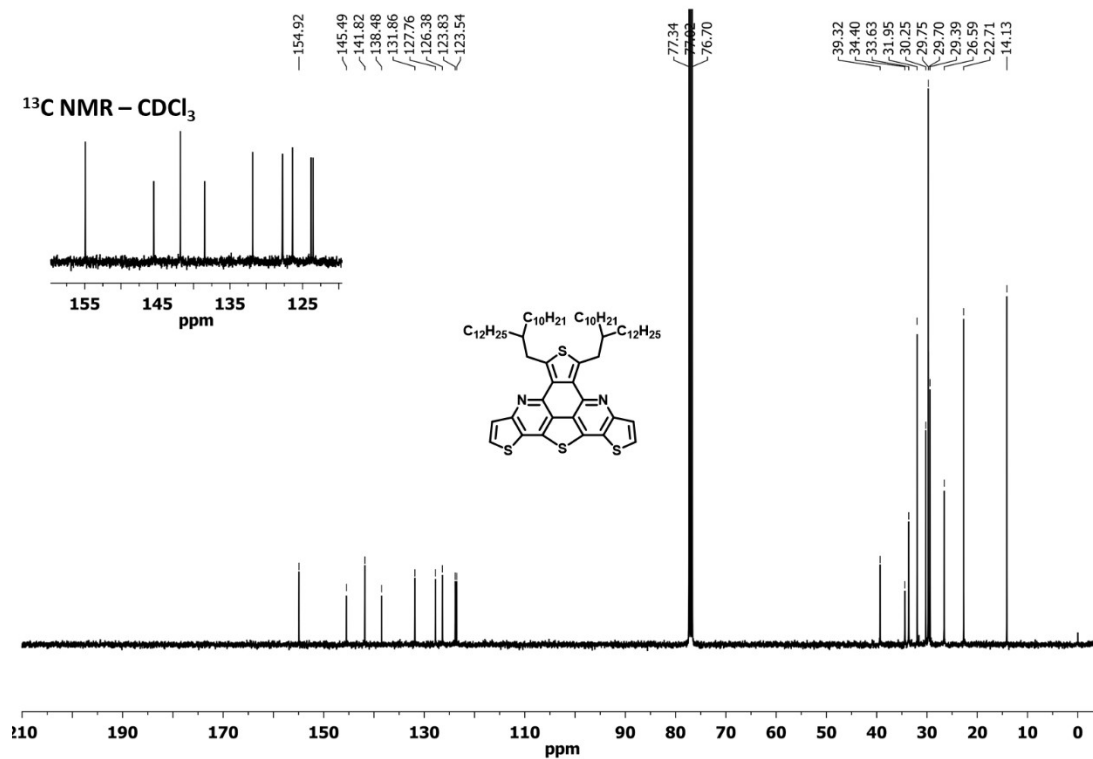
3.15. **Figure S15:** ^{13}C NMR spectra of di-tert-butyl ((5,7-bis(2-decyltetradecyl)-4,8-dioxo-4H,8H-benzo[1,2-c:4,5-c']dithiophene-1,3-diyl)bis(thiophene-2,3-diyl))dicarbamate (3b)



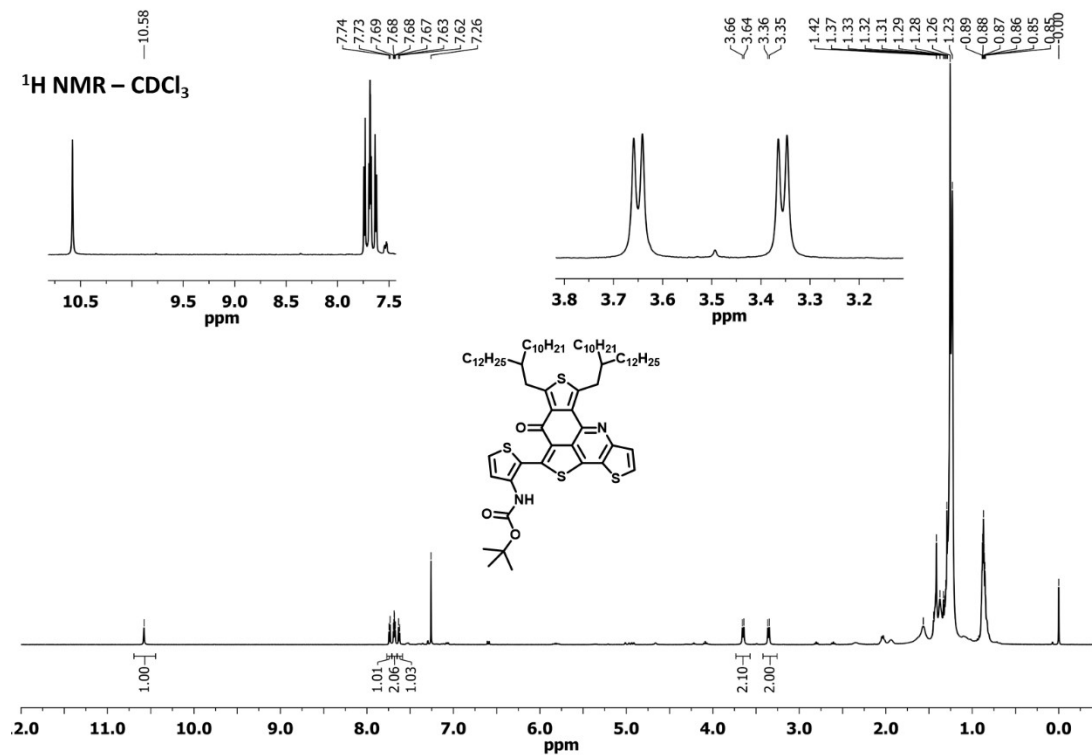
3.16. **Figure S16:** ^1H NMR spectra of 5,7-bis(2-decyltetradecyl)tetrathieno[2,3-b:3',4'-f:3'',2''-j:2''',3''',4''',5'''-lmn][4,7]phenanthroline (TTP2)



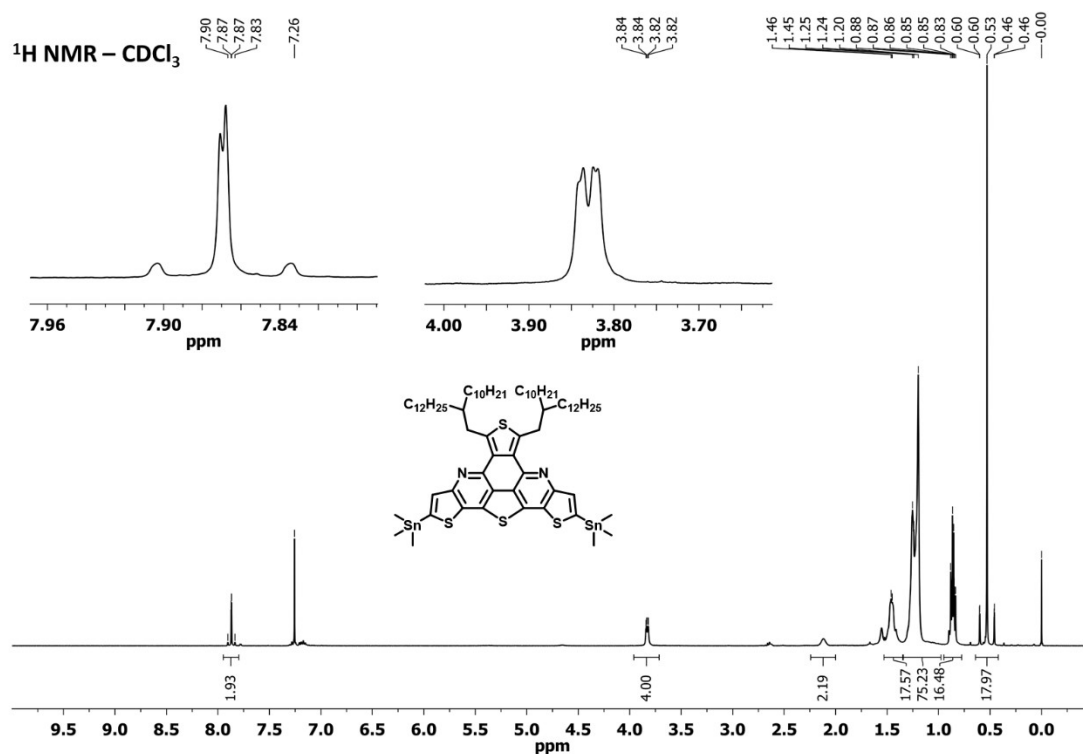
3.17. **Figure S17:** ^{13}C NMR spectra of 5,7-bis(2-decyltetradecyl)tetrathieno[2,3-b:3',4'-f:3'',2''-j:2''',3''',4''',5'''-lmn][4,7]phenanthroline (TTP2)



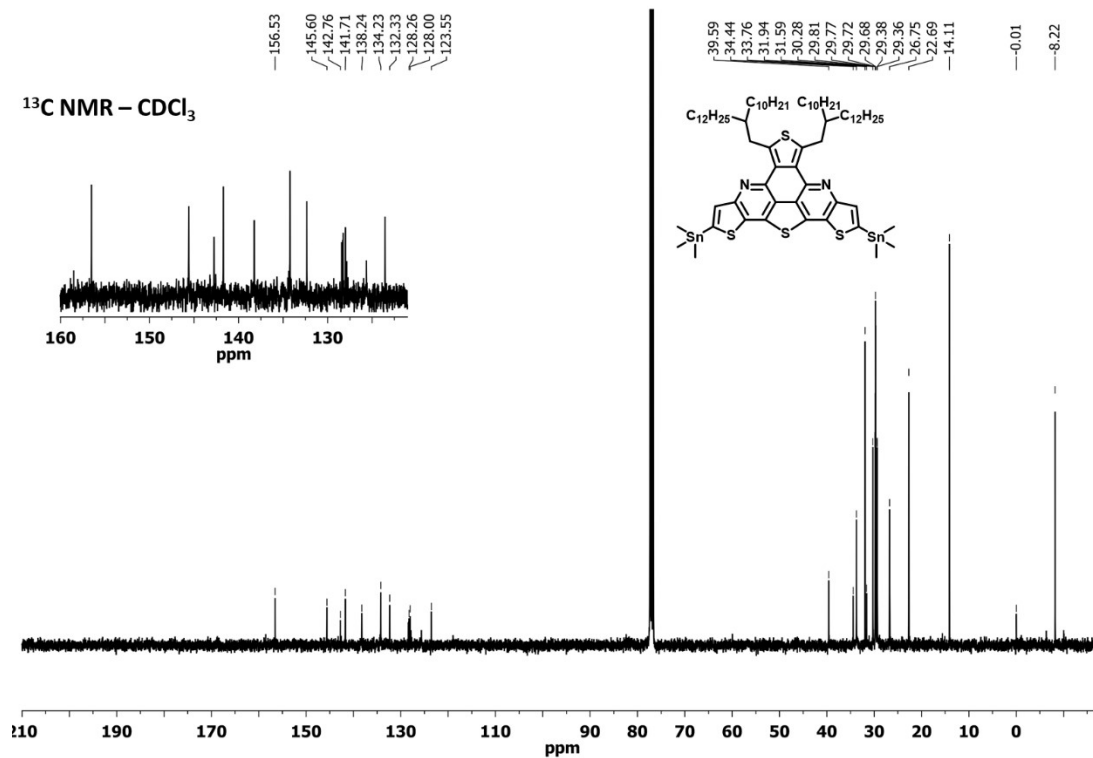
3.18. Figure S18: ^1H NMR spectra of tert-butyl (2-(7,9-bis(2-decyltetradecyl)-6-oxo-6H-trithieno[3,2-b:2',3',4'-de:3'',4''-h]quinolin-5-yl)thiophen-3-yl)carbamate



3.19. **Figure S19:** ^1H NMR spectra of 5,7-bis(2-decyltetradecyl)-2,10-bis(trimethylstannyl)tetrathieno[2,3-b:3',4'-f:3'',2''-j:2''',3''',4''',5'''-lmn][4,7]phenanthroline (TTP2-Sn)



3.20. Figure S20: ^{13}C NMR spectra of 5,7-bis(2-decyltetradecyl)-2,10-bis(trimethylstannyl)tetrathieno[2,3-b:3',4'-f:3'',2''-j:2''',3''',4''',5'''-lmn][4,7]phenanthroline (TTP2-Sn)



4. Gel permeation chromatography

4.1. Figure S21: GPC analysis of PTPP-BDT

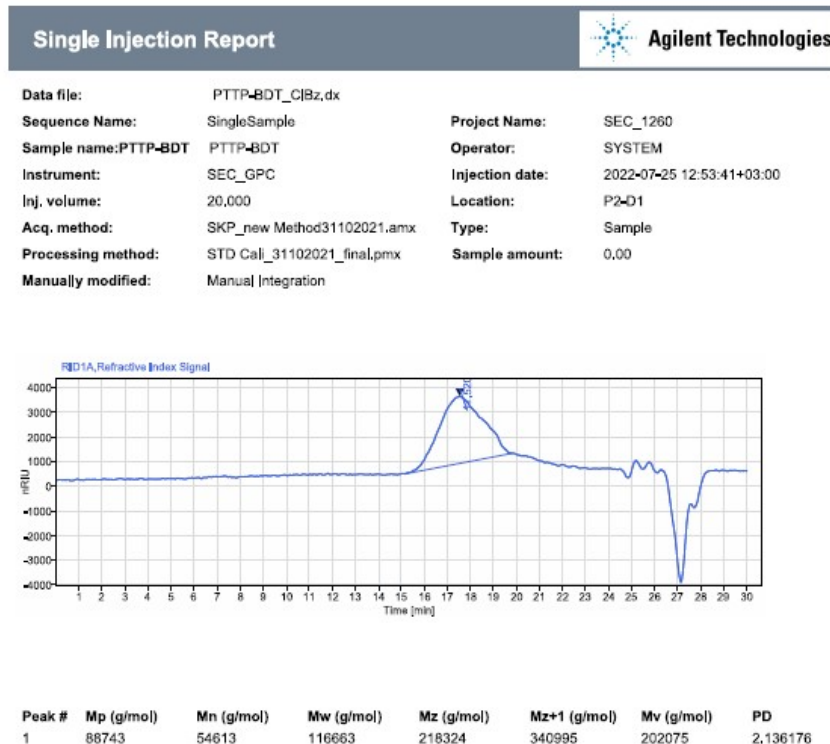


Table S1. Conditions explored for one pot acid catalyzed deprotection and ring fusion

No.	Acid	Conditions	Half fusion	Full fusion	Decomposition
1	HCl/Toluene	0°C -RT-Reflux overnight	Very low	No	Yes
2	TFA/Toluene	Rt-Reflux 48h	Minor	Trace	Yes
3	CF ₃ SO ₃ H/Toluene	Rt-Reflux 48h	Trace	Major	Trace

5. Photovoltaic Measurements

5.1. Table S2. Optimisation of D/A concentration for PTPP-BDT:Y6 based Organic Solar Cells

Concentration	PCE (%)	Voc (mV)	Jsc (mA/cm ²)	FF (%)
15mg/mL	2.87	720	8.9	44.68

18mg/mL	2.85	728	9	43.17
<u>21mg/mL</u>	2.96	711	10.2	40.5
24mg/mL	2.76	679	10.2	39.7

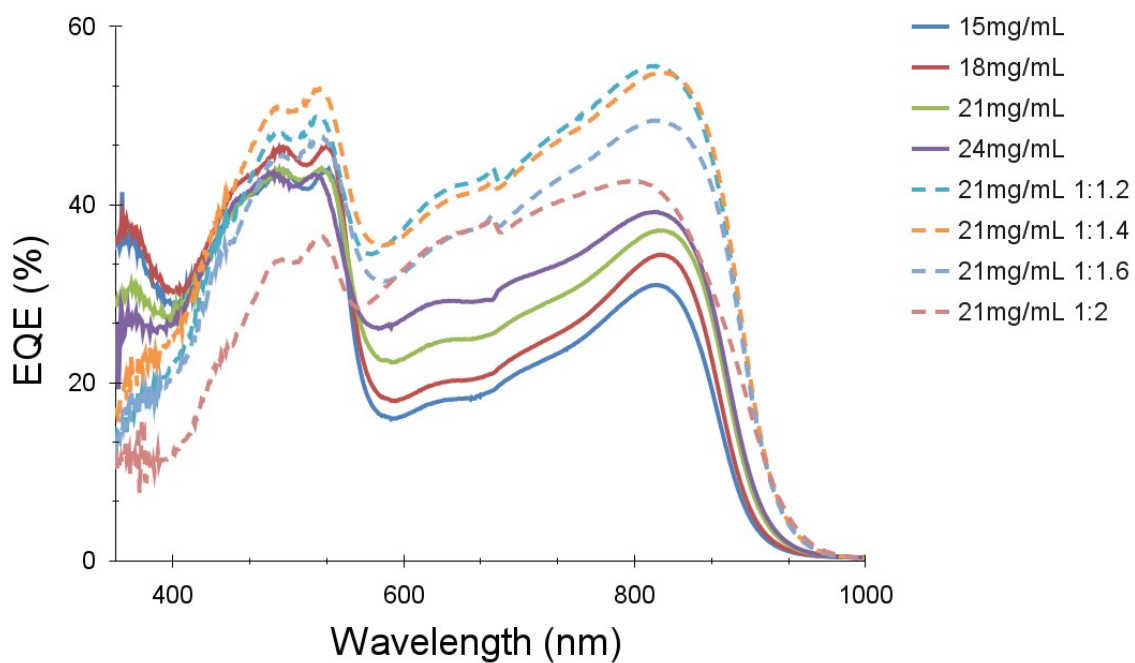
5.2. **Table S3.** Optimisation of D/A ratio for PTPP-BDT:Y6 based Organic Solar Cells

Ratio	PCE (%)	Voc (mV)	Jsc (mA/cm²)	FF (%)
1:1	2.96	711	10.2	40.5
<u>1:1.2</u>	2.95	661	10.9	41
1:1.4	2.81	648	10.6	40.9
1:1.6	2.63	655	10	40
1:2	2.2	629	8.8	39.5

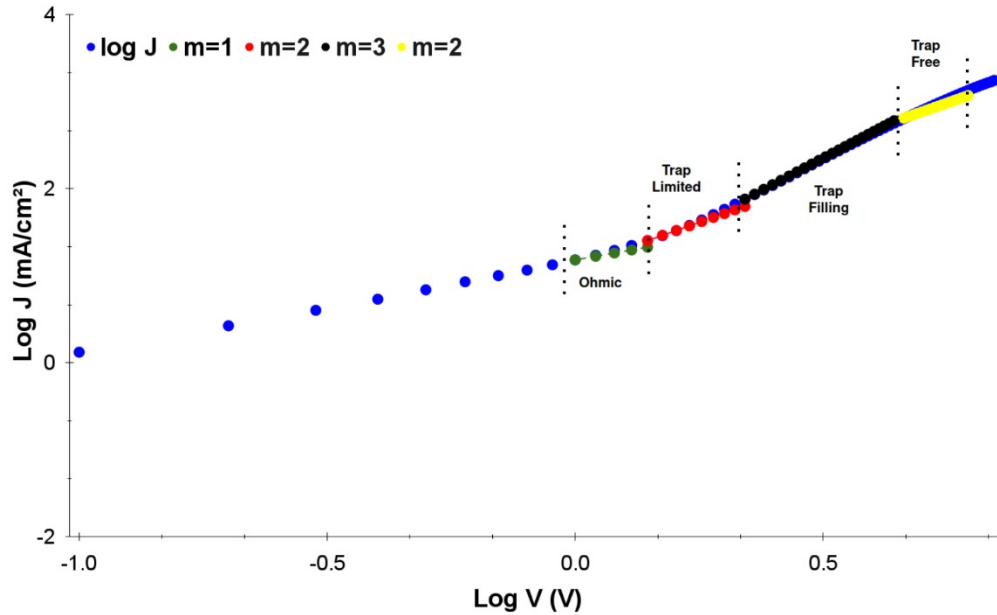
5.3. **Table S4.** Photovoltaic performance of PBDB-T:Y6 BHJ solar cells. Blend concentration was 19.8 mg/mL with D/A ratio of 1:1.2

PCE (%)	Voc (mV)	Jsc (mA/cm ²)	FF (%)
7.8	718	18.1	60

5.4. **Figure S22.** External Quantum Efficiency spectra of fabricated Organic Solar Cells with different D/A concentration and D/A ratio.



5.5. **Figure S23.** Fitting of double logarithmic dark J-V curve of PTPP-BDT based hole only devices. Hole mobility was measured by considering Trap-free region where the slope of curve was 2.



5.6. **Figure S24.** Photovoltaic characterisation of devices based on novel PTPP-BDT1:Y6 vs reference PBDB-T:Y6 over time. Values are normalised. (a) Power conversion efficiency (b) Open circuit voltage (c) Short circuit current (d) Fill Factor of fabricated devices

